

Self-healing of Engineered Cementitious Composites under Reversed and Sustained Loading Conditions

Sina Mahmoodi ¹ and Pedram Sadeghian ²

¹ *Department of Civil and Resource Engineering, Dalhousie University, 1360 Barrington Street, Halifax, NS, B3H 4R2, Canada. Email: Sina.Mahmoodi@dal.ca (corresponding author)*

² *Department of Civil and Resource Engineering, Dalhousie University, 1360 Barrington Street, Halifax, NS, B3H 4R2, Canada. Email: Pedram.Sadeghian@dal.ca*

ABSTRACT:

The present study investigates the effects of reversed and sustained flexural loading cycles on the repeatability of self-healing in Engineered Cementitious Composites (ECC). The experimental work is designed to test three cases of normal (REF), reverse (REV) and reverse-sustained (RES) loading and three different exposure conditions of tap water, sea water, and open air. A total of 27 prism specimens (100×100×350 mm) were fabricated, and a four-point bending test was used for flexural load application at different stages and to further measure the recovery in mechanical properties. The research is proposed to elaborate on the positive/negative impact of compression cycle on the self-healing of cracks. Ultrasonic Pulse Velocity (UPV) test was carried out before and after each loading and the wave travel time was compared as an indicator of healing efficiency. To monitor crack propagation patterns and crack widths, Digital Image Correlation (DIC) technique was used. To further analyze the mineralogy and microstructure of the healing products, X-ray Diffraction (XRD) test was conducted on two groups of tap water and sea water exposures. Concluding results proved that sea water and tap water are suitable environments for autogenous self-healing process.

Furthermore, reverse loading cycles were demonstrated to impact the self-healing results and should be considered for repeatable self-healing evaluations.

DOI: <https://doi.org/10.1002/suco.202100214>

KEYWORDS: ECC, Self-healing, Sustained Loading, Reverse Loading, Seawater

1. INTRODUCTION

Self-healing mechanisms have been introduced into cementitious materials over the last twenty years to enhance the durability and increase the lifetime of the infrastructure while diminishing the repair cost and labor (Ferrara et al., 2018; Huang, Ye, Qian, & Schlangen, 2016; Van Tittelboom & De Belie, 2013). Autogenous and Autonomous mechanisms are the two major methods of self-healing in cementitious materials (De Belie et al., 2018). While autogenous method is mainly focused on the further hydration of unhydrated particles and crystallization of calcium carbonate (Edvardsen, 1999; Ramm & Biscop, 1998), autonomous healing is more versatile with representing mechanisms such as bacteria-based self-healing (Gupta, Dai Pang, & Kua, 2017; Jonkers, Thijssen, Muyzer, Copuroglu, & Schlangen, 2010; Vijay, Murmu, & Deo, 2017), and encapsulation techniques of adhesive agents (Feiteira, Gruyaert, & De Belie, 2016; Souradeep & Kua, 2016; Van Tittelboom, De Belie, Van Loo, & Jacobs, 2011). The existing literature on self-healing concrete is broad, and the results are promising, however, the application of self-healing mechanisms has not yet reached the industrial gates. For instance, the highly alkaline environment of concrete, added to the high temperature during the initial hydration, is considered a big challenge for bacteria based self-healing mechanisms. (Das, Mishra, Yu, & Leung, 2019; Gardner, Lark, Jefferson, & Davies, 2018; Lee & Park, 2018; Zhang, Wang, & Han, 2020). To establish a better connection with industry, some researchers suggested implementing “Robustness criteria” as a filter to identify and accredit the practical methods to be used in sustainable infrastructure (V. C. Li & Herbert, 2012; V. C. Li & Yang, 2007; Tang, Kardani, &

Cui, 2015; Wang et al., 2019). The robustness criteria implies that every mechanism needs to meet at least six criteria including shelf life, pervasiveness, quality, reliability, versatility, and repeatability to be justified for application in sustainable infrastructure. Among them, the repeatability i.e., the ability of the mechanism to be able to trigger not only once, but upon multiple cracking over the estimated lifetime raises a significant challenge. Due to the inevitable repetition of external loads/harsh environments that induce cracking over the lifetime of the infrastructure, accompanied by the localized cracking behavior of cementitious composites, the repeatability of the mechanisms that mainly rely on the formation of low-strength and low-toughness healing products (e.g. Polymorphs of $CaCO_3$ such as aragonite or vaterite) is threatened (Rodriguez-Navarro, Elert, & Ševčík, 2016). It also questions the micro and macro encapsulation techniques when the healing agents are released after the first cracking and hardened inside the cracks space, taking away the healing capability for any further damage that may occur (V. C. Li & Herbert, 2012; Mahmoodi & Sadeghian, 2019), even though there have been studies on the encapsulation of flexible polymers which are able to adhere to the crack walls even when cracks were opened further (Feiteira et al., 2016). Moreover, the repeatability of self-healing mechanism is a crucial asset for justifying the life cycle cost of self-healing mechanisms for industry (Van Breugel, 2007). To help obtain a repeatable self-healing mechanism in concrete, a set of physical, chemical and environmental conditions are suggested (M. Li & Fan, 2016). Fibers that bridge the cracks to control the damage, high unreacted ingredients that promote the formation of materials such as Calcium Silicate Hydrate (C-S-H) or strong crystals, and presence of moisture in the surrounding environment are suggested to be most effective (Cuenca & Ferrara, 2020; Cuenca, Tejedor, & Ferrara, 2018; Özbay et al., 2013; Sahmaran, Yildirim, Noori, Ozbay, & Lachemi, 2015; Snoeck & De Belie, 2016; Yildirim, Alyousif, Şahmaran, & Lachemi, 2015).

Engineered Cementitious Composite (ECC) that possesses two-third of the aforementioned properties, has been of high interest to researchers for its repeatability properties. ECC is a special category of High-Performance Fiber-Reinforced Cementitious Composites (HPFRCC), introduced by Li (V. C. Li, 1993). The main characteristic of ECC that distinguishes it from other fiber-reinforced cementitious composites is its deflection-hardening behavior that is the result of a synergetic interaction between fibers, cementitious matrix and the interface (Yıldırım, Keskin, Keskin, Şahmaran, & Lachemi, 2015). Adding to its unique structural behavior, the high fractional volume of micro-fibers that limits the crack widths, plus the high portions of Supplementary Cementitious Material (SCM) such as fly ash that remain unreacted during the initial hydration, not only promotes self-healing, but suggests the fact that it can introduce repeatable self-healing into the infrastructure (Herbert & Li, 2013; V. C. Li & Herbert, 2012; Sahmaran et al., 2015; Yildirim et al., 2015).

Sahmaran et al. (Sahmaran et al., 2015) studied the repeatability of self-healing in ECC through the Resonant Frequency (RF) and Rapid Chloride Permeability (RCP) tests. He concluded that ECC specimens could recover up to 85% of their initial RF measurements, even after six repetitive preloadings. However, it should be considered that the crack widths in his test were limited to 190 µm, and wet/dry cycles were provided during curing periods. Snoeck and De Belie (Snoeck & De Belie, 2016) suggested implementing Super Absorbent Polymers (SAP) in ECC to help with the water supply during the curing time under repeated loads, however, Herbert and Li (Herbert & Li, 2013) claimed that ECC is capable of maintaining its self-healing functionality after multiple damage in the natural environment. To see the effect of different loading conditions, Yildirim et al. (Yildirim et al., 2015) assessed the self-healing behavior of ECC under increasing sustained loading cycles. After 180 days of initial curing, the prism specimens were subjected to 40% of their ultimate flexural capacity, and 10% increase was applied every 30 days for 5 cycles. Ultrasonic Pulse Velocity (UPV)

test and recovery of mechanical properties were used to measure the healing efficiency over the test period. It was stated that the deflection results were more adversely affected by progressive sustained loading than the healing process, indicating the influence of loading condition on the healing process. To study a more conventional case of concrete, Cuenca et. al (Cuenca et al., 2018) replaced ECC with a normal Fiber Reinforced Concrete (FRC) to keep the fibers in action, and changed the fly ash as the source of late hydration with Crystalline Admixtures (CA) which are water soluble additives that produce crystals during the fresh and hardened state. They studied the repeatability of self-healing under three different exposure conditions of water immersion, open air, and wet/dry cycles for a year and concluded that effect of CA persists after repeated cracking-healing cycles, but it highly depended on its surrounding environment, as almost no healing was observed in the open air. In another attempt, Cuenca and Ferrara (Cuenca & Ferrara, 2020) tried to correlate fracture toughness parameters from mechanical recovery to crack sealing capacity index of FRC with CA under repeated cracking-healing cycles. They concluded that the exposure condition and the crack width play a dominant role in the healing efficiency under repeated loading.

The present experimental study is designed to investigate the repeatability of self-healing in ECC with addressing two decisive parameters, namely: loading condition and exposure condition. As it was concluded in the previous studies, different loading conditions can have a significant impact on the healing process. To further investigate that, a set of reverse loading cycles were used in this study. Along, cases of sustained loading were carried out to assess the crack stability effects on the repeatability of self-healing. Furthermore, since the surrounding environment has been reported numerous times as a determinant factor on the repeatability of self-healing, and also due to direct contact of many of our infrastructure with the ocean, it is essential to study the effects of sea water on

the repeatability of the healing process. Therefore, exposure to tap water, sea water and open air is considered in this study to investigate the effect of exposure condition on the healing process.

2. RESEARCH SIGNIFICANCE

The magnitude and direction of external forces that are transferred into a structural concrete member varies, depending on the member's role and position in the structure. Moreover, some external forces act at multiple directions (e.g., wind load), while some are hardly predictable (e.g., seismic load). That implies different events for a partially healed crack. Almost all of the available literature on the repeatability of self-healing has considered the repetitive external cycles as loading cycles that open up the partially healed cracks to the pre-cracking level or higher. However, there is a chance that the partially healed cracks undergo a compression state where they are forced to close due to the external forces. This applies a new condition to the healing process that has not been studied yet. The main scope of this study is to investigate the positive/negative impacts of this new condition on the functionality of the healing process in ECC during multiple damaging. The results will determine the necessity of considering reverse cycles which induce a compressive stress on the elements.

3. EXPERIMENTAL PROGRAM

The experimental program implemented in this study aims to measure the repeatability of self-healing mechanism in ECC under reverse loading cycles. For this purpose, 27 ECC prism specimens with a single mix design were fabricated and afterward, tested under tension and compression cycles. Four-point bending test was selected for loading cycles and also to measure the self-healing through regaining of mechanical properties. Digital Image Correlation (DIC) technique was used to monitor the loading stages and to measure Crack Mouth Opening Displacement (CMOD), and Ultrasonic Pulse Velocity (UPV) test was employed to assess the healing efficiency of cracks during the test

period. To study the mineralogy of the formed healing products, X-Ray Diffraction (XRD) test was conducted on the healing products scratched from the face of the cracks after final loading.

3.1. Material Properties and Specimen Fabrication

A single ECC mix design incorporating Class-F fly ash (FA), type GU Portland cement (C), micro-silica sand (S) with an average aggregate size of $225\ \mu\text{m}$, water (W), high-range water-reducing admixture (HRWRA) and polyvinyl alcohol (PVA) fibers with a nominal tensile strength of 1100-1400 MPa, diameter of $38\ \mu\text{m}$, length of 8 mm and specific gravity of 1.3 was used in this study. Table 1. provides details on the portions of the mix design. Water to cementitious material ratio (W/FA+C) was 0.27. The compressive strength of the adopted mix design was measured by means of compression test on three standard cylindrical specimens at the age of 7-day and 28-day and the results were 28.5 ± 0.9 MPa and 40.0 ± 1.2 MPa, respectively. Since large crack formations are investigated in this experiment, the relatively high FA/C ratio of 2.2 was selected to promote the healing efficiency of ECC by late hydration (Herbert & Li, 2013; Hung & Su, 2016; Özbay et al., 2013); also, it reduces the cement portion in the mixture.

Since moderate dispersion of PVA micro-fibers is an effective issue on ECC properties, a planetary blade mixer was used to mix ECC ingredients properly. First, fly ash, cement, and micro-silica sand were mixed for 5 minutes. Then, water was added and gradually after that, PVA fibers were added and mixed for 5 minutes. Finally, the HRWRA was added, and the mixing process continued for another 5 minutes. The fabricated ECC was poured into wooden molds to make $100\ \text{mm} \times 100\ \text{mm} \times 350\ \text{mm}$ ECC prisms. After keeping the fabricated specimens under plastic sheets in a curing room with 95% relative humidity for 24 hours, the wooden forms were removed and the ECC prisms were placed back again in the curing room up to the age of 28 days. After the moisture curing was completed, the specimens were taken out of the curing room and prepared for pre-cracking. The

specimens were kept in an ambient temperature (22°C) and humidity (RH=74%) for 4 months before the first pre-cracking started.

3.2. Test Plan and Exposure Conditions

The objective of this study is to investigate the repeatability of self-healing in ECC after a series of loading cycles. The novelty is to use a reverse loading cycle as the repeating cycle between pre-cracking and final loading cycles to determine the effect of compression stress on the healing process of partially healed cracks. Also, since the sustained state of loading keeps the crack width to open wider and disturbs the healing process by making the cracks unstable, the effects of applying a set of sustained loading conditions on the healing efficiency was studied in parallel to repeatability.

For this purpose, three groups of specimens labeled as REF (Reference group), REV (Reverse loading group), and RES (Reverse-Sustained loading group) were planned to be tested. A summary of the test plan and studied exposure conditions is presented in Table.2. The first loading cycle applied to all three groups was pre-cracking. This step was conducted using four-point bending test after the initial curing period was completed (see section 3.2.1). Generally, pre-cracking is a force/displacement-controlled test in which the specimen is cracked up to a specific percentage of its ultimate force/displacement capacity. After testing 6 dummy specimens under four-point bending test, it was observed that the continuation of post-linear behavior (deflection-hardening stage) is highly dependent on the weak point of cracking, crack propagation pattern and the fiber orientation and dispersion at the crack locations (M. Li & Fan, 2016; Zhou et al., 2012). Therefore, in this study the specimens were pre-cracked up to a point where a visually distinguishable crack (which was measured by DIC to be between 200-250 μ m, after unloading) was observed on the specimens. This high deflection was selected purposefully so that fibers between cracks will not be able to interfere with the UPV measurements. For a few ECC prisms, reaching to this point was also accompanied by

a small load reduction, indicating that the specimen is now experiencing post-peak behavior (tension softening stage). However, for most of other specimens, the load was increasing when a distinct crack was observed. This provided an excellent set of data to evaluate the healing efficiency of ECC in terms of regaining the mechanical properties during both deflection hardening/softening stages.

After pre-cracking, the specimens in group RES were put inside a sustained loading fixture to experience the final mid-span deflection that they have been subjected to under the pre-cracking stage. Hence, the amount of mid-span relaxation after unloading the pre-cracking force was measured for these specimens by means of LVDT and DIC and then applied to them using the sustained fixture as shown in Fig. 1.c. A digital displacement gauge was fixed perpendicular to the bottom of the specimens at the mid-span to measure the mentioned displacement. The load was applied with an ACDelco digital torque wrench shown in Fig 1.b, which was calibrated three times with a load cell before the tests and compatible results were obtained (Fig 1.a). In this step of the test, the specimens in group RES undergo a tension (T) state, where cracks are being opened up (see Fig. 1.d).

To study the effects of different exposure conditions on healing process, after the pre-cracking step, specimens were exposed to three different curing conditions, including tap water, sea water, and open air (RH=74%) for four months, which provided the cracks with enough time to heal partially or entirely. The ion concentration of the sea water used in the investigation is presented in Table.3. Upon completing the first curing period, the repeating cycle which was selected to be a reverse cycle in this study, was applied through a force-controlled four-point bending process to groups REV and RES. The specimens in group REV were placed upside down in the loading setup and were subjected to four-point bending. The purpose of this loading cycle was to apply compression stress on the partially healed cracks, and the criteria for selecting its loading limit was to have the least impact on the mechanical properties of the other side of the cracked prisms. Therefore, based on the pre-cracking

results of actual specimens, 10 kN was selected as the compression cycle loading limit to be applied in this stage, which as demonstrated in Fig. 2, will predict to affect the other side of the prisms linearly, therefore minor impact on the mechanical properties is generated. For group RES, the specimens were put upside down in the sustained fixtures and the compression (C) cycle was applied with the torque wrench (see Fig. 1.e). As mentioned, the torque wrench was calibrated using a pancake load cell and the equivalent torque for 10 kN load was obtained to be 25 N.m.

The specimens were all placed again in the exposure conditions that they have been experiencing for the last four months. After another two months of curing period, all groups were taken out and tested under four-point bending until failure¹. The self-healing process for each specimen was studied individually and also as a group, and results were obtained and compared as relative values. To validate the results and also to have different ECC behaviors studied in each case, three specimens were tested for each case of study, making a total number of 27 specimens.

3.2.1. Four-point bending test

In order to induce controlled flexural cracks on ECC prisms and also to evaluate healing efficiency through the recovery of mechanical properties, four-point bending test was carried out for all loading stages of this test. It is the nature of the four-point bending system to provide a maximum moment region between the middle loads, promoting the ECC multi-cracking behavior in this region; hence real ECC behavior is investigated. An Instron 8501 load cell with a 100 kN capacity was used to apply a loading rate of 0.5mm/min, and one data was recorded per 0.5 seconds. Mid-span deflection was measured via an LVDT placed in the middle of the test setup. The specimen's dimensions and apparatus configuration were in accordance with ASTM C78 (C78M-18) (See Fig. 3). It is worth

¹ The timeline of the experiment was modified from the original plan due to COVID-19 pandemic.

noting that the test setup was placed upside down in the actual tests due to the upward load exertion of the Instron.

3.2.2. DIC Analysis

Digital Image Correlation (DIC) is an optical measuring technique that determines the displacement field of the surface of an object under loading. The method tracks the movement of a grey value patterns (speckle pattern) on the surface of the specimen at any point of time with regards to a desired reference pattern. Test requires a camera to record the test process and software to further analyze the results (See Fig. 4). In this study, DIC analysis was conducted using the software GOM Correlate 2018. A Canon 750D equipped with a 35 mm lens was adopted to record the test for all stages of loading. The surfaces that were supposed to be recorded were first sprayed with a white paint and after drying, painted with a black speckle spray. The camera was placed at a distance of approximately 500 mm from the specimen and at a perpendicular angle to the front side. The technique was used to determine crack propagation patterns, measure the crack mouth opening and also to measure the mid-span relaxation after unloading which was used in applying sustained load with the fixture. Since there was only one camera used to collect data and to avoid any error with DIC readings, the DIC measurements were calibrated with LVDT data initially and a correction factor was generated which was further used for post data processing.

3.2.3. UPV test

Ultrasonic Pulse Velocity (UPV) method is a simple Non-Destructive Testing (NDT) technique used to assess the mechanical properties of concrete, such as strength and also to detect the defects such as cracks. The test measures the travel time of a compressional ultrasonic wave over a known path length through concrete. As shown in Fig. 5, the presence of a crack would increase the travel time of the wave, yet filling that crack with healing products would cause the time to decrease ($T_2 > T_3 \geq T_1$).

This change in transmission time, which is a result of pre-cracking and crack healing, is used as an evaluation parameter to measure the healing efficiency over the test period.

The testing scheme is illustrated in Fig. 6. Based on ACI 228.2R (228.2R-13) and ASTM C597 (C597-16) recommendations, two transducers with a natural frequency of 54 kHz and 50 mm diameter were employed to transmit and receive compression wave signals. A Pundit UPV tester with the time-sensitivity range of (μ s) and a pulse voltage of 110 V was used in this study. The transducers were placed on the smaller facet of the ECC prisms such that the top of them were at the center of the facet and the bottoms were leveled. Concrete surface was cleaned and sanded by sandpaper before attaching the sensors and honey was used for smoother connection. The test was started from the virgin state of the specimens onwards and the travel times were recorded before and after every loading cycle and compared as a relative parameter indicating the healing efficiency.

4. RESULTS AND DISCUSSIONS

4.1. Recovery of Mechanical Properties

After testing 27 ECC prism specimens under four-point bending, it was observed that different mechanical behavior is likely to be achieved after that first cracking occurs. As shown in Fig. 7, the specimens demonstrate different deflection-hardening/softening properties in pre-cracking stage, which can be related to the location and size of the initial flaw that usually generates the main crack and also the orientation and dispersion of fibers at the flaws in each ECC specimen (Lu, Li, & Leung, 2018). This issue caused a range of peak strengths and deflections that, if were supposed to be used for self-healing evaluation purposes, then there was a high chance of self-healing results being manipulated by the pre-cracking loading process. On the other hand, the initial stiffness showed consistency in the pre-cracking step, furthermore, it deals more directly with crack opening stage. As autogenous self-healing progresses, the newly generated healing products start to fill the cracks, which

mostly happens at the nucleation sites provided by the dense pack of PVA fibers at crack locations (Kan & Shi, 2012). It is reasonable to believe that the formation of new products around the fibers increases the initial stiffness of the section via increasing fibers' bond with the cementitious matrix (Ma, Herbert, Ohno, & Li, 2019). Therefore, Stiffness recovery ratio (R_S) was selected in this study as the representative of recovery in mechanical properties, and is defined as follows:

$$R_S = \frac{\text{Initial stiffness of final loading}}{\text{Initial stiffness of precracking}} \leq 1 \quad \text{Eq.1}$$

By comparing the results of the stiffness recovery ratio (R_S) for REF and REV groups shown in Fig.8, it can be stated that applying a compression cycle to the cracks that have already undergone some healing process decreases the recovery of stiffness. This trend was observed in all exposure conditions, more significantly in tap water and sea water with a %39 and 8% decrease, respectively. This contradicts the idea that applying a compression cycle to a crack will help the autogenous healing process by closing the crack and reducing the space required for healing production. That could be the case if the compression cycle was applied before the healing process initiated, but apparently, applying forces that compress the partially healed crack (such as a series of reverse loading cycles) destroys the structure of formed healing products (e.g. CaCO_3 and $\text{Mg}(\text{OH})_2$), and reduces the amount of stiffness that could be recovered over time. Other than that, the interfacial transition zone (ITZ) between the healing products inside the cracks and the concrete matrix could be damaged by the compression loading. Moreover, the fibers that usually provide nucleation sites for the healing products and are in the center of generated self-healing products may have been squeezed, leading to impaired fiber-bridging capacity.

The trend was more adversely affected by the sustained loading condition in RES group. Results in Fig. 8 show that a series of reverse loading cycles where the loading condition is sustained and therefore cracks are larger, minimizes the chances of improved autogenous self-healing process. With

applying a sustained condition to the reverse loading cycles, the stiffness recovery ratio decreased by 13%, 49% and 55%, for sea water, tap water and open air conditions, respectively. It is worth mentioning that in this investigation, the cracks widths for the selected specimens in sustained condition of tension were around 500 μ m, which is an extremely high value for ECC.

Generally, sea water proved to be a better medium for autogenous self-healing, rather than tap water or open air. Presence of different ions dissolved in sea water, such as Mg^{2+} , helps with formation of new healing products such as brucite ($Mg(OH)_2$) that can promote crack healing efficiency of ECC in addition to calcite ($CaCO_3$). According to Fig. 8 ECC specimens cured in sea water, reached to 80% of their initial stiffness in REF group, where there was one pre-loading and one final loading, and no reverse cycle. In addition, a comparison of results between REF and RES groups shows that loading condition is less impactful on sea water exposure with %21 decrease, however there was a %69 and %57 decrease in specimens exposed to tap water and open air.

4.2. UPV results

Ultrasonic Pulse Velocity test was carried out for all ECC specimens throughout the test plan. Table. 4 summarizes the travel times of the compression waves measured at different stages of cracking and healing. To accredit the results, three specimens were examined for each case, and the average of the results is presented. As predicted, the time values for the intact ECC prisms are almost the same (84-85 μ s), showing a constant velocity of ~4.2 km/s that is generally considered in the range of good quality concrete (Leslie & Cheesman, 1949; Saint-Pierre, Philibert, Giroux, & Rivard, 2016). After the initial pre-cracking, the travel time for all cases increased, indicating the presence of the cracks in the specimens. The results for the two cases of REF and REV are quite similar since the pre-cracking stage is identical for both conditions. However, the specimens in group RES demonstrated higher travel times due to the sustained loading that eliminated the relaxation after unloading.

With the first exposure condition of four months finished, all specimens were taken out of their curing condition and tested for UPV measurement. At this stage, the UPV values showed improvement in the wave travel time in all specimens, indicating that cracks are being filled with healing products. This improvement in wave travel time was more obvious in specimens exposed to tap water and sea water as expected. Even though, it should be mentioned that another cause for the improvement of UPV values in the specimens cured in tap water and sea water at this stage could be the densification and continuous hydration of the concrete matrix due to the penetration of the moisture from the surrounding environment. After applying the reverse compression cycle to the specimens in groups REV and RES, the UPV test was conducted again to determine the compression state's effect on partially healed cracks. Results tabulated in Table. 3 prove that in group REV, where tension cracks are relatively small (~200-250 μm), compressing the cracks will not significantly impact wave travel time. Although cracks are being closed by the compression force, yet the applied force will affect negatively on the structure of the healing products formed during the first curing period. Since cracks are wider in group RES (~500 μm) and there is a less chance for the formation of autogenous healing products, the compression cycle's effect is more significant on closing the cracks, rather than the destruction of newly formed products.

To investigate the overall effect of different loading conditions on the self-healing efficiency, UPV Recovery ratio (R_U) was defined as follows:

$$R_U = 1 - \left(\frac{\text{Final UPV} - \text{Intact UPV}}{\text{Intact UPV}} \right) \leq 1 \quad \text{Eq.2}$$

As demonstrated in Fig. 9, the numbers obtained for R_U are in the range of 0.80 – 1.00, which are very close and relatively high. However, as described in section 3.2.3. the compression wave will travel through the shortest path in concrete, which in this study was observed to be the crack mouth where formation of autogenous healing products (e.g. calcite) is more likely to occur (Sisomphon,

Copuroglu, & Koenders, 2012). As a reason, a high UPV recovery ratio will not necessarily confirm a totally filled crack. Regardless, aligned with the results of last section, R_U values prove that sea water is the most effective environment in terms of filling the cracks with ~95% recovery in all groups, while open air showed the least recovery in RES condition with ~87%. Compared to results of the previous section, the difference between the values of tap water and sea water is less in the UPV measurements than stiffness recovery ratio, which could be resulted by the different mineralogy of the healing products or the fact that in UPV measurements, the waves can travel from any filled section which might not contribute to recovery of fiber stiffness.

Considering the fact that the only difference between REV and REF groups is the compression cycle that was applied to REV group in the process of self-healing, the R_U results indicate a slight decrease in the values for REV in all three exposure conditions. It could be claimed that while the compression cycle in REV group closes the crack width, it compresses and crushes the newly formed autogenous healing products. This issue is more obvious in specimens exposed to open air condition, where the healing products inside the cracks are assumed to be more brittle due to lack of moisture.

4.3. XRD analysis

To investigate the microstructure and material characteristics of autogenous healing products in this experimental program, X-Ray Diffraction (XRD) test was performed on the powder samples scratched from inside of cracks in ECC specimens after the final loading. Two groups of tap water and sea water exposures were selected for this test due to their higher efficiency in terms of crack healing and also to determine the different healing products formed in these conditions. Fig. 10 demonstrates XRD patterns of samples for ECC in sea water and tap water obtained using an X-Ray diffractometer with Cu Ka radiation and 2theta ranging between 0 to 80 degrees.

As predicted, brucite ($\text{Mg}(\text{OH})_2$) was observed in ECC specimens submerged in sea water, which indicates the presence of Mg ions in sea water, also confirms the formation of additional healing products that enhance the autogenous healing efficiency in this exposure condition. A mix of brucite and calcite layers is also formed in the sea water exposed samples, which was also reported in previous research (Danner, Hjorth Jakobsen, & Geiker, 2019). Calcite was observed in both groups as a premier product of autogenous self-healing in later ages, indicating the presence of dissolved carbonate ions in tap and sea water. Quartz (SiO_2) peaks are also determined in the samples, which could be related to the silica in the sand and FA used in ECC mixtures.

5. CONCLUSION

The presented experimental program was carried out to evaluate the improved autogenous self-healing efficiency of ECC prism specimens under instant and sustained reverse loading cycles. Three different exposure conditions of sea water, tap water, and open air were selected as the surrounding environment of specimens for the duration of the tests. Recovery of mechanical properties, UPV test and XRD analysis were used to evaluate the self-healing efficiency in this investigation. The main objective of this research was to determine whether applying a compression cycle in between repetitive tension cycles needs to be considered while assessing the repeatability of autogenous self-healing mechanism. Stiffness recovery ratio R_S was defined based on mechanical properties obtained from four-point bending tests. The values indicate that applying a compression cycle on partially healed cracks can have adverse effects on the stiffness recovery, such that it destroys the brittle structure of newborn healing products (e.g., CaCO_3), and reduces the amount of stiffness that could be recovered over time. RES group that represented a sustained reverse loading condition on ECC prisms proved lower recovery ratios in terms of stiffness. UPV results also confirm this behavior in ECC specimens. It can be stated that while the repeatability of self-healing in ECC is yet an issue

under investigation, it should be considered that compression cycles and sustained loading condition will reduce the efficiency of improved autogenous self-healing in partially healed cracks.

Furthermore, X-Ray Diffraction (XRD) analysis was carried out on healing products collected from inside the healed cracks. Formation of additional healing products such as brucite was reported in specimens exposed to sea water, which enhanced the efficiency of self-healing in ECC. R_S results show about 80% recovery in flexural stiffness for specimens in the REF group that were submerged in sea water for six months. This recovery ratio was found to be around 73% and 64% for REV and RES groups, respectively. Apparently, sea water is a favorable condition for the improved autogenous self-healing in ECC material, even at high displacements. XRD patterns also confirmed the presence of calcite which is a well-established autogenous healing product.

Further investigation is suggested to be conducted on the structural aspects of improved autogenous self-healing in ECC with more emphasis on different loading amplitudes and durations, that represent real service conditions of concrete infrastructure. Microscopic level investigation of cracks and the healing products could help verify the results of the tested regime.

ACKNOWLEDGEMENTS

This research was undertaken thanks in part to funding from the Canada First Research Excellence Fund, through the Ocean Frontier Institute, Dalhousie University, Halifax, NS, Canada.

REFERENCES

- 228.2R-13, A. C. I. A. Report on Nondestructive Test Methods for Evaluation of Concrete in Structures. *American Concrete Institute: Farmington Hills, MI, USA, 2013.*
- C78M-18, A. C. Standard Test Method for Flexural Strength of Concrete (Using Simple Beam with Third-Point Loading). *ASTM International, West Conshohocken, PA, USA, 2018.*

C597-16, A. *Standard Test Method for Pulse Velocity Through Concrete*.

Cuenca, E., & Ferrara, L. (2020). Fracture toughness parameters to assess crack healing capacity of fiber reinforced concrete under repeated cracking-healing cycles. *Theoretical and Applied Fracture Mechanics*, 106, 102468.

Cuenca, E., Tejedor, A., & Ferrara, L. (2018). A methodology to assess crack-sealing effectiveness of crystalline admixtures under repeated cracking-healing cycles. *Construction and Building Materials*, 179, 619-632.

Danner, T., Hjorth Jakobsen, U., & Geiker, M. R. (2019). Mineralogical sequence of self-healing products in cracked marine concrete. *Minerals*, 9(5), 284.

Das, A. K., Mishra, D. K., Yu, J., & Leung, C. K. (2019). Smart Self-Healing and Self-Sensing Cementitious Composites—Recent Developments, Challenges, and Prospects. *Advances in Civil Engineering Materials*, 8(3), 554-578.

De Belie, N., Gruyaert, E., Al-Tabbaa, A., Antonaci, P., Baera, C., Bajare, D., . . . Jefferson, T. (2018). A review of self-healing concrete for damage management of structures. *Advanced materials interfaces*, 5(17), 1800074.

Edvardsen, C. (1999). Water permeability and autogenous healing of cracks in concrete. In *Innovation in concrete structures: Design and construction* (pp. 473-487): Thomas Telford Publishing.

Feiteira, J., Gruyaert, E., & De Belie, N. (2016). Self-healing of moving cracks in concrete by means of encapsulated polymer precursors. *Construction and Building Materials*, 102, 671-678.

Ferrara, L., Van Mullem, T., Alonso, M. C., Antonaci, P., Borg, R. P., Cuenca, E., . . . Roig-Flores, M. (2018). Experimental characterization of the self-healing capacity of cement based materials and its effects on the material performance: a state of the art report by COST Action SARCOS WG2. *Construction and Building Materials*, 167, 115-142.

- Gardner, D., Lark, R., Jefferson, T., & Davies, R. (2018). A survey on problems encountered in current concrete construction and the potential benefits of self-healing cementitious materials. *Case studies in construction materials*, 8, 238-247.
- Gupta, S., Dai Pang, S., & Kua, H. W. (2017). Autonomous healing in concrete by bio-based healing agents—A review. *Construction and Building Materials*, 146, 419-428.
- Herbert, E. N., & Li, V. C. (2013). Self-healing of microcracks in engineered cementitious composites (ECC) under a natural environment. *Materials*, 6(7), 2831-2845.
- Huang, H., Ye, G., Qian, C., & Schlangen, E. (2016). Self-healing in cementitious materials: Materials, methods and service conditions. *Materials & Design*, 92, 499-511.
- Hung, C.-C., & Su, Y.-F. (2016). Medium-term self-healing evaluation of Engineered Cementitious Composites with varying amounts of fly ash and exposure durations. *Construction and Building Materials*, 118, 194-203.
- Jonkers, H. M., Thijssen, A., Muyzer, G., Copuroglu, O., & Schlangen, E. (2010). Application of bacteria as self-healing agent for the development of sustainable concrete. *Ecological engineering*, 36(2), 230-235.
- Kan, L.-l., & Shi, H.-s. (2012). Investigation of self-healing behavior of Engineered Cementitious Composites (ECC) materials. *Construction and Building Materials*, 29, 348-356.
- Lee, Y. S., & Park, W. (2018). Current challenges and future directions for bacterial self-healing concrete. *Applied microbiology and biotechnology*, 102(7), 3059-3070.
- Leslie, J., & Cheesman, W. (1949). An ultrasonic method of studying deterioration and cracking in concrete structures. *Journal of the American Concrete Institute*, 21(1), 17-36.
- Li, M., & Fan, S. (2016). Designing repeatable Self-healing into cementitious materials.

- Li, V. C. (1993). From micromechanics to structural engineering-the design of cementitious composites for civil engineering applications.
- Li, V. C., & Herbert, E. (2012). Robust self-healing concrete for sustainable infrastructure. *Journal of Advanced Concrete Technology*, 10(6), 207-218.
- Li, V. C., & Yang, E.-H. (2007). Self healing in concrete materials. In *Self healing materials* (pp. 161-193): Springer.
- Lu, C., Li, V. C., & Leung, C. K. (2018). Flaw characterization and correlation with cracking strength in Engineered Cementitious Composites (ECC). *Cement and Concrete Research*, 107, 64-74.
- Ma, H., Herbert, E., Ohno, M., & Li, V. C. (2019). Scale-linking model of self-healing and stiffness recovery in Engineered Cementitious Composites (ECC). *Cement and Concrete Composites*, 95, 1-9.
- Mahmoodi, S., & Sadeghian, P. (2019). *Self-healing concrete: a review of recent research developments and existing research gaps*. Paper presented at the 7th International Conference on Engineering Mechanics and Materials, Laval, QC, Canada.
- Özbay, E., Sahmaran, M., Yücel, H. E., Erdem, T. K., Lachemi, M., & Li, V. C. (2013). Effect of sustained flexural loading on self-healing of engineered cementitious composites. *Journal of Advanced Concrete Technology*, 11(5), 167-179.
- Ramm, W., & Biscop, M. (1998). Autogenous healing and reinforcement corrosion of water-penetrated separation cracks in reinforced concrete. *Nuclear Engineering and Design*, 179(2), 191-200.
- Rodriguez-Navarro, C., Elert, K., & Ševčík, R. (2016). Amorphous and crystalline calcium carbonate phases during carbonation of nanolimes: implications in heritage conservation. *CrystEngComm*, 18(35), 6594-6607.

- Sahmaran, M., Yildirim, G., Noori, R., Ozbay, E., & Lachemi, M. (2015). Repeatability and pervasiveness of self-healing in engineered cementitious composites. *ACI Materials Journal*, *112*(4), 513.
- Saint-Pierre, F., Philibert, A., Giroux, B., & Rivard, P. (2016). Concrete quality designation based on ultrasonic pulse velocity. *Construction and Building Materials*, *125*, 1022-1027.
- Sisomphon, K., Copuroglu, O., & Koenders, E. (2012). Self-healing of surface cracks in mortars with expansive additive and crystalline additive. *Cement and Concrete Composites*, *34*(4), 566-574.
- Snoeck, D., & De Belie, N. (2016). Repeated autogenous healing in strain-hardening cementitious composites by using superabsorbent polymers. *Journal of Materials in Civil Engineering*, *28*(1), 04015086.
- Souradeep, G., & Kua, H. W. (2016). Encapsulation technology and techniques in self-healing concrete. *Journal of Materials in Civil Engineering*, *28*(12), 04016165.
- Tang, W., Kardani, O., & Cui, H. (2015). Robust evaluation of self-healing efficiency in cementitious materials—A review. *Construction and Building Materials*, *81*, 233-247.
- Van Breugel, K. (2007). *Is there a market for self-healing cement-based materials*. Paper presented at the Proceedings of the first international conference on self-healing materials.
- Van Tittelboom, K., & De Belie, N. (2013). Self-healing in cementitious materials—A review. *Materials*, *6*(6), 2182-2217.
- Van Tittelboom, K., De Belie, N., Van Loo, D., & Jacobs, P. (2011). Self-healing efficiency of cementitious materials containing tubular capsules filled with healing agent. *Cement and Concrete Composites*, *33*(4), 497-505.

- Vijay, K., Murmu, M., & Deo, S. V. (2017). Bacteria based self healing concrete—A review. *Construction and Building Materials*, *152*, 1008-1014.
- Wang, X., Yang, Z., Fang, C., Han, N., Zhu, G., Tang, J., & Xing, F. (2019). Evaluation of the mechanical performance recovery of self-healing cementitious materials—its methods and future development: a review. *Construction and Building Materials*, *212*, 400-421.
- Yildirim, G., Alyousif, A., Şahmaran, M., & Lachemi, M. (2015). Assessing the self-healing capability of cementitious composites under increasing sustained loading. *Advances in Cement Research*, *27*(10), 581-592.
- Yıldırım, G., Keskin, Ö. K., Keskin, S. B., Şahmaran, M., & Lachemi, M. (2015). A review of intrinsic self-healing capability of engineered cementitious composites: Recovery of transport and mechanical properties. *Construction and Building Materials*, *101*, 10-21.
- Zhang, W., Wang, D., & Han, B. (2020). Self-healing concrete-based composites. In *Self-Healing Composite Materials* (pp. 259-284): Elsevier.
- Zhou, J., Qian, S., Ye, G., Copuroglu, O., van Breugel, K., & Li, V. C. (2012). Improved fiber distribution and mechanical properties of engineered cementitious composites by adjusting the mixing sequence. *Cement and Concrete Composites*, *34*(3), 342-348.

Table. 1. ECC mix design for 1 m³

Ingredients	FA	C	S	W	PVA	HRWRA
Weight (kg)	823	375	435	318	26	3

Table. 2. ECC test plan and exposure conditions. (T) represents the sustained condition where cracks are under tension and (C) represent the sustained condition where cracks are under compression

Group name	UPV	Pre-cracking	UPV	Exposure (4 months)	UPV	Reverse loading	UPV	Exposure (2 months)	UPV	Final loading
REF				Tap water		N/A		Tap water		
				Sea water				Sea water		
				Air dry				Air dry		
REV				Tap water				Tap water		
				Sea water				Sea water		
				Air dry				Air dry		
RES				Tap water (T)				Tap water (C)		
				Sea water (T)				Sea water (C)		
				Air dry (T)				Air dry (C)		

Note: Three specimens were tested for each case of study, making a total number of 27 specimens.

Table. 3. Concentration of major constituents in sea water based on the salinity of the collected area

	At salinity 30%					
	Na ⁺	K ⁺	Mg ²⁺	Ca ²⁺	Cl ⁻	HCO ₃ ⁻
Weight (g/kg)	9.24	0.34	1.10	0.35	16.58	0.11

Table. 4. UPV test results

Group name	Exposure conditions	UPV results (μs)					
		Intact ECC specimens	After pre-cracking	1 st exposure condition (4 months)	After finishing the 1 st curing period	After applying compression cycle to REV and RES	2 nd exposure condition (2 months)
REF	Tap water	84	95			90	
	Sea water	85	96	90		88	
	Open air	84	96	94		93	
REV	Tap water	84	95	90		91	89
	Sea water	84	95	90		90	88
	Open air	84	96	92		92	94
RES	Tap water	85	98	91	89	89	
	Sea water	84	99	90	89	89	
	Open air	84	98	93	96	95	

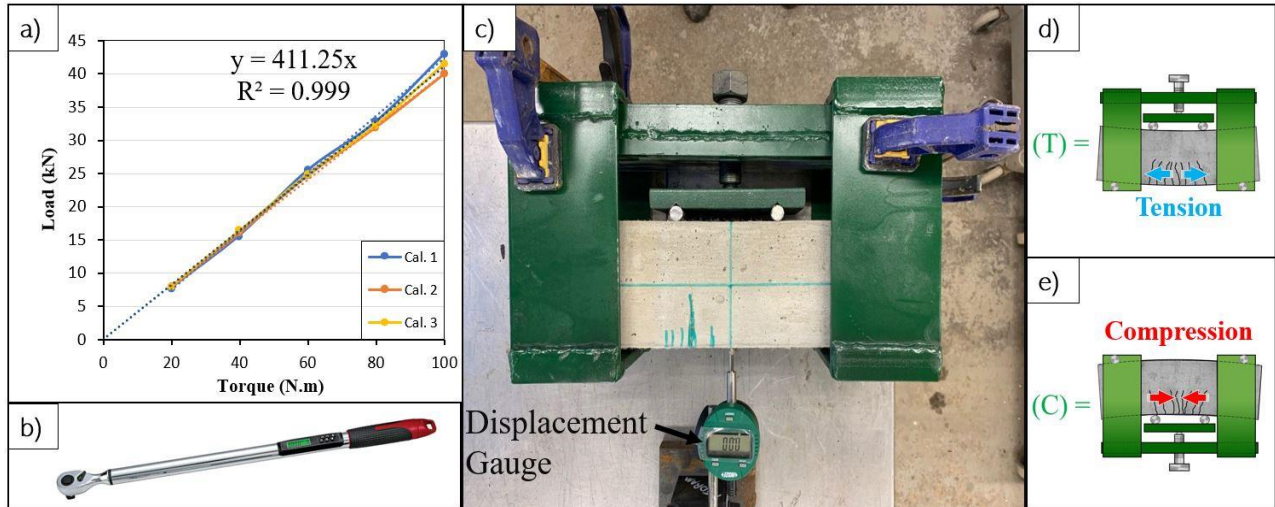


Fig. 1. Sustained loading fixture setup tools and test conditions, a) Torque vs. load calibration of the torque wrench, b) AC Delco digital torque wrench, c) sustained loading fixture clamped to the table and displacement gauge fixed at the mid-span, d) cracks under sustained tension and, e) cracks under sustained compression

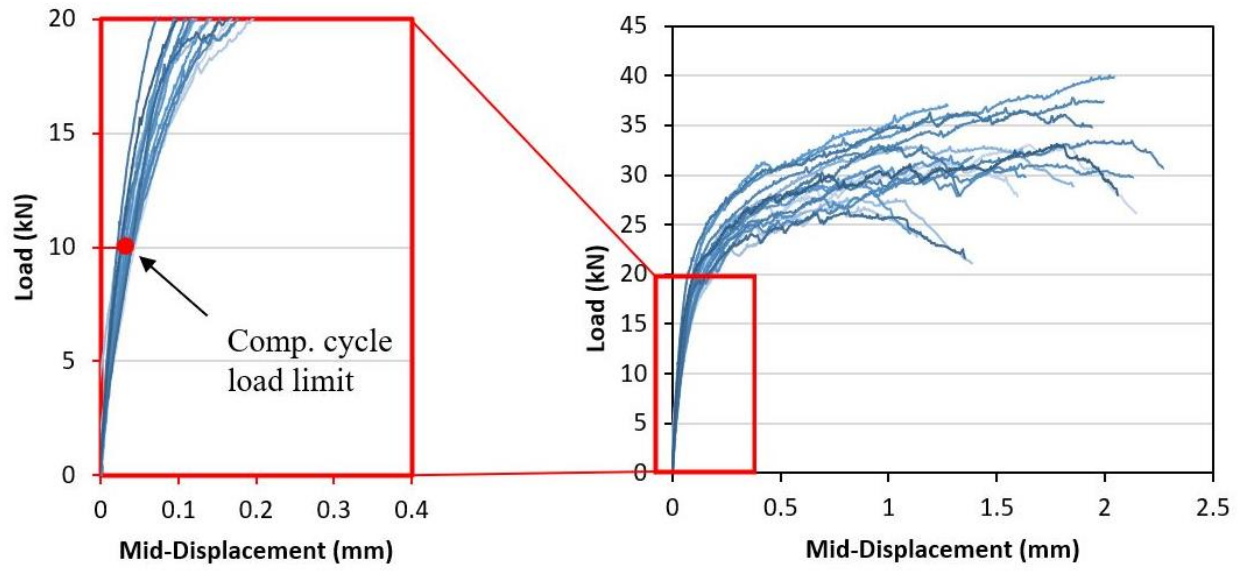


Fig. 2. Using pre-cracking results of ECC prisms to determine the compression cycle load limit

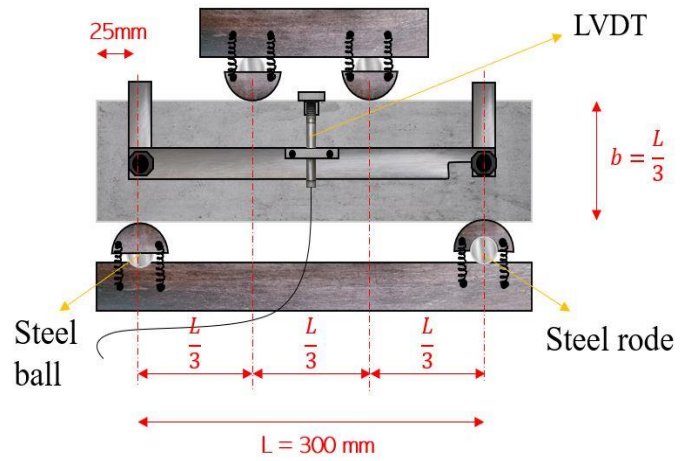


Fig. 3. Four-point bending test apparatus and dimensions

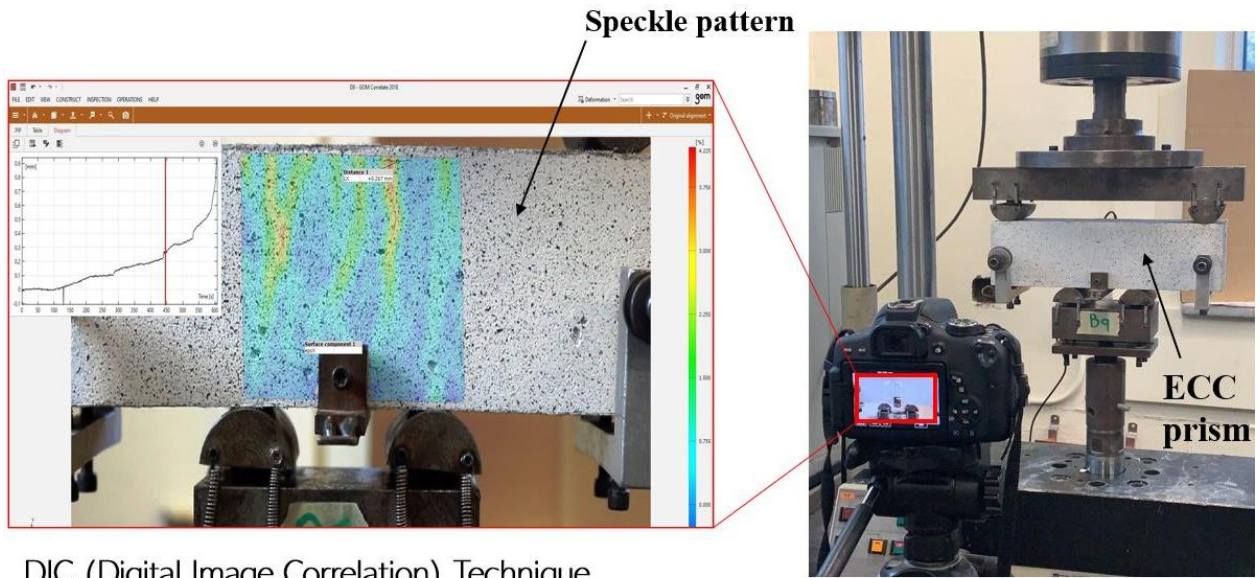


Fig. 4. Recording four-point bending test to use in DIC analysis

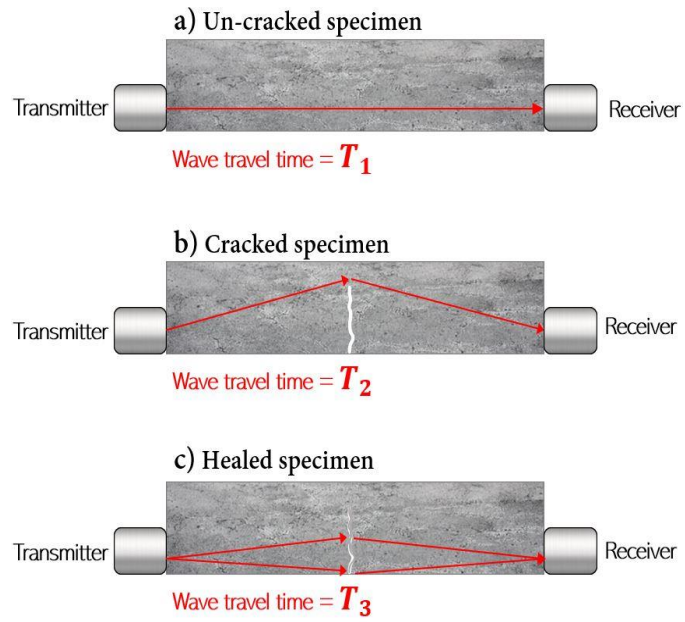


Fig. 5. Wave travel path through concrete prisms; a) un-cracked specimen, b) cracked specimen and, c) healed specimen.

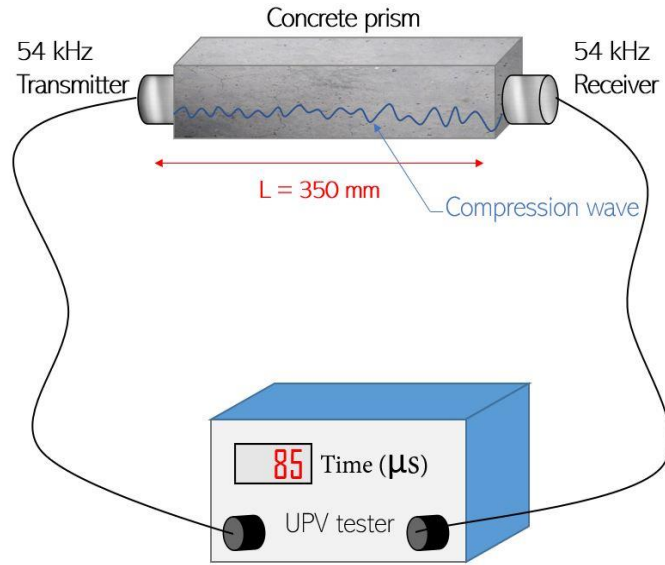


Fig. 6. UPV test setup

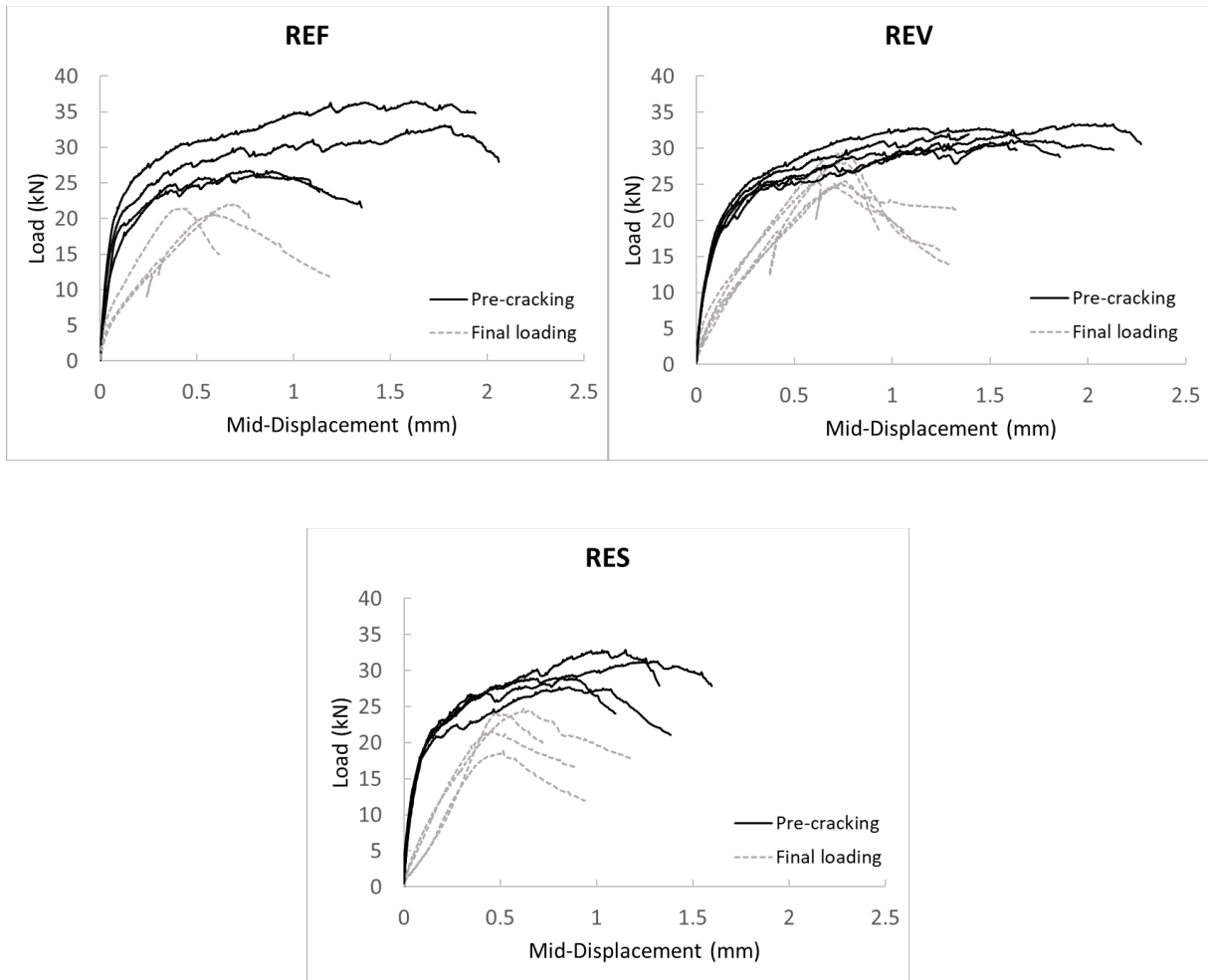


Fig. 7. Load vs. Midspan deflection of pre-cracking and final loading for groups REF, REV, and RES

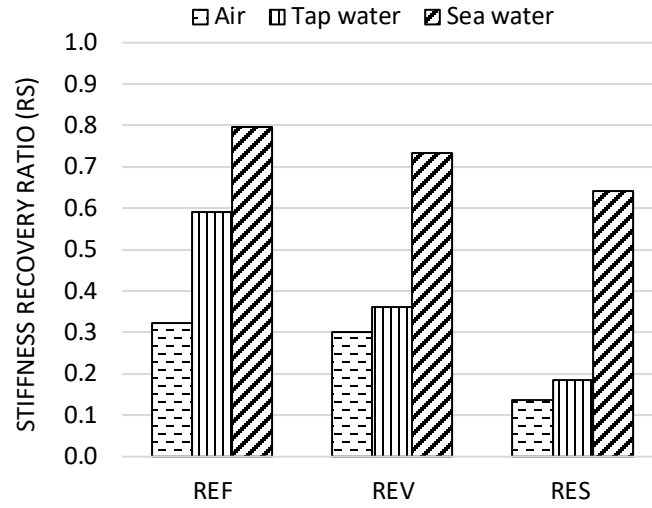


Fig. 8. Stiffness recovery ratio (R_S) of groups REF, REV, and RES exposed to different environmental conditions

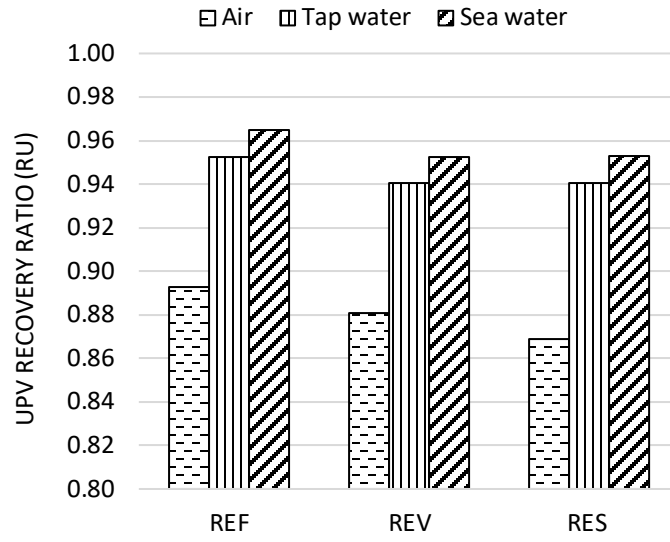


Fig. 9. UPV recovery ratio (R_U) of groups REF, REV, and RES exposed to different environmental conditions

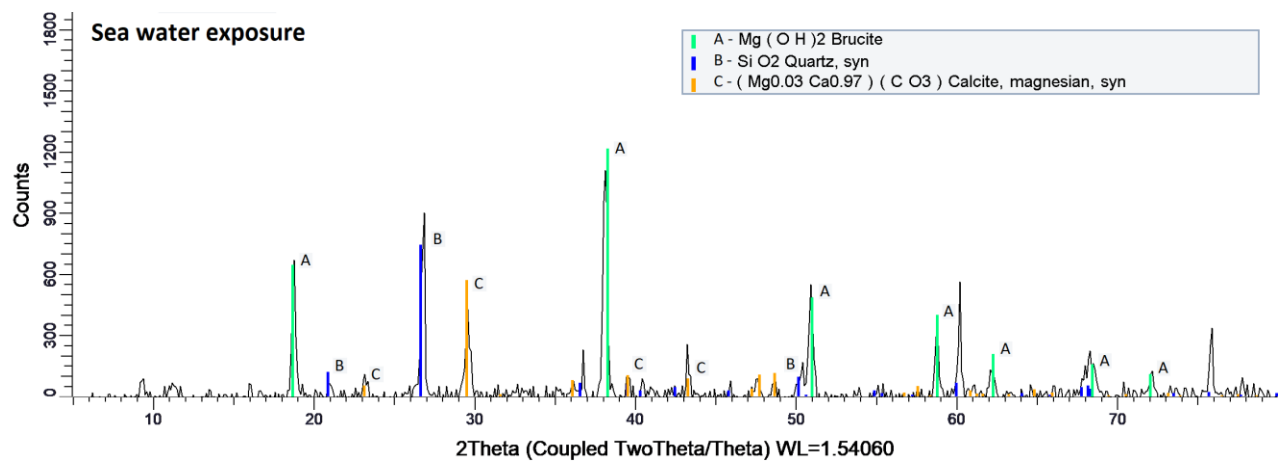
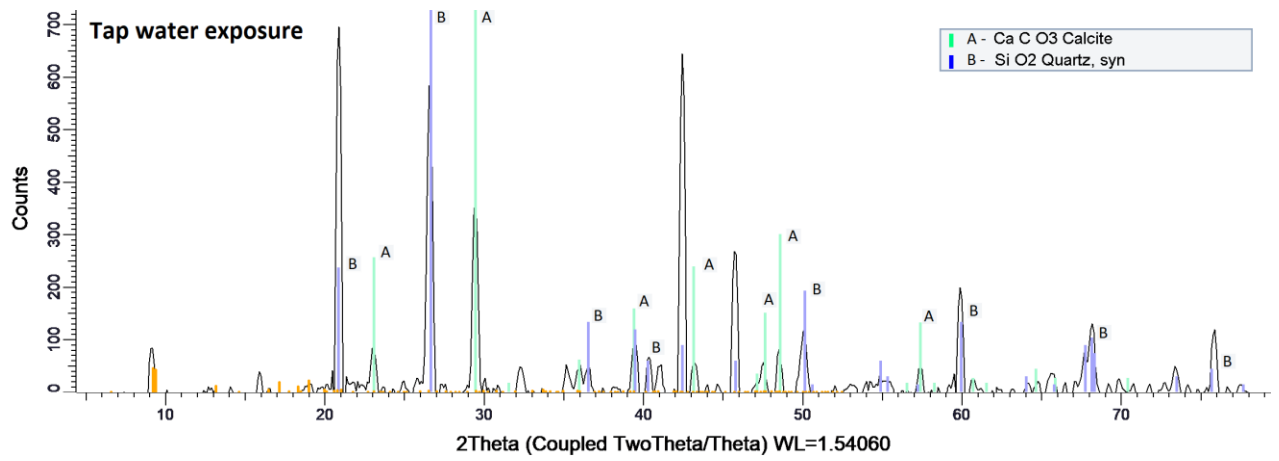


Fig. 10. XRD analysis of ECC specimens exposed to tap water and sea water condition